scientific reports

OPEN

PNMA1 mediates melphalam chemoresistance in retinoblastoma via promoting DNA repair

Longge Sun, Zhaokang Xu, Xin Zhang, Xing Du, Guanghui Li & Yuanyuan Guo✉

Retinoblastoma (RB) is the most common malignant eye tumor in children. Cytotoxic drugs like melphalam often cause significant side effects and acquired resistance in RB treatment. Here, the impact of Paraneoplastic Ma1 (PNMA1) on RB progression and chemotherapy resistance was investigated. A series of bioinformatics methods were used for differential expression genes and drug resistance genes screening. Western blot was performed for the detection of genes expression. CCK-8 and EdU staining were assessed for cell viability. Clone formation and TUNEL staining were examined for cell viability and apoptosis. Wound healing and transwell assays were analyzed for the cell migrated and invasive abilities. Immunofluorescence was observed for γ-H2AX expression. Colorimetric PARP/ Apoptosis Assay was used for PARP activity. PNMA1 was upregulated in RB tumor tissues, and high expression of PNMA1 promotes RB cells' chemoresistance to melphalam, while downregulation of PNMA1 reversed chemoresistance in resistant cells. Furthermore, the mechanism by which PNMA1 mediated chemoresistance to melphalam, discovered that PNMA1 might facilitate melphalam resistance through the c-myc-mediated DNA damage repair pathway. PNMA1 functions as a tumor-promoting factor in retinoblastoma and may regulate melphalam resistance through the upregulation of the c-myc gene and the involvement in DNA damage repair.

Keywords Retinoblastoma, PNMA1, Melphalan, Chemoresistance, DNA repair

Retinoblastoma (RB), the most common malignant eye tumor in children, is characterized by its tendency for early metastasis, with a 3-year survival rate of only 57.3% in low-income countries[1]. Recent advances in targeted chemotherapy and multimodal treatment strategies have significantly improved the overall cure rate for RB patients[2,3]. However, challenges persist, particularly for advanced RB, mainly due to tumor progression following chemotherapy-induced resistance[4]. The expression of multidrug resistance proteins (MRPs), enhanced drug efflux mechanisms, and the presence of tumor stem cells have been implicated as potential causes of RB tumor resistance[5–7]. Consequently, identifying effective therapeutic targets for RB resistance has become an urgent issue in current research.

Paraneoplastic Ma1 (PNMA1) is a member of the PNMA family, which consists of at least 15 members[8]. PNMA1-3 are closely related to paraneoplastic disorder, and they interact with Bax to mediate apoptosis signals[8,9]. Studies have shown that PNMA1 was involved in apoptosis signaling in mouse neurons[10]. In pancreatic cancer, PNMA1 has been demonstrated to act as an oncogene by activating the PI3K/AKT and MAPK/ERK pathways[11]; in hepatocellular carcinoma, PNMA1 regulates the WNT/β-catenin pathway to promote cell proliferation and epithelial-mesenchymal transition (EMT)[12]. However, the role of PNMA1 in retinoblastoma remains largely unexplored.

In this study, that was investigated, the upregulation of PNMA1 in RB tissues and its role in mediating melphalam resistance through the regulation of myc gene expression and DNA damage repair. This finding holds significant implications for RB tumor treatment.

Methods
Data download
Download the retinoblastoma RNA-seq data from the GEO database: GSE97508, GSE110811 and GSE229598, which include tumor samples (6 cases in GSE97508, 28 cases in GSE110811, and 114 cases in GSE229598) and normal retinal tissues (3 cases in GSE97508 and 3 cases in GSE110811). The datasets were combined, and the sva package[13] was used to normalize the original data. The DEGs were screened in the batch calibrated test set using the limma package[14]. selected |log2 fold change FC | > 1 and adj. p. value < 0.05 as truncation criteria.

Department of Ophthalmology, The Second People's Hospital of Jinan, No.148, Jingyi Road, Jinan 250000, Shandong Province, China. ✉email: 18963091069@163.com

Gene set enrichment analysis (GSEA)

On the grounds of the median risk score, the RB samples were assigned into high-risk and low-risk subsets. GSEA was proceeded utilizing GSEA software version 4.1.0, with 'h.all.v2023.2.Hs.symbols.gmt' gene set utilized as the reference. The Bonferroni correction method was implemented to adjust for comparisons in GSEA evaluations, while non-parametric statistical approaches were employed for datasets that violated the assumption of normal distribution as assessed by Shapiro-Wilk testing.

Cell culture

SO-RB50 cell line used in this study were obtained from Procell and cultured in Dulbecco's Modified Eagle Medium(DMEM) (Procell, Wuhan, China) supplemented with 10% FBS (Procell, Wuhan, China) at 37 °C and 5% CO_2. All cells were tested negative for Mycoplasma contamination and authenticated by short tandem repeat (STR) fingerprinting at Guangzhou Cellcook Biotech Company. When the cell confluence was about 80%, digestive passage was performed with trypsin.

Transfection

Transfection was carried out during the logarithmic growth phase of the cells. According to the conditions of the manufacturers, serum-free medium and lipo8000 (Beyotime) mixture were used to mix 5nM siRNA (si-NC: 5'-UUCUCCGAACGUGUCACGU-3', si-PNMA1-1: 5'-GCAGAGAUGCUAAACUAUATT-3', si-PNMA1-2: 5'- GCGGUUGAUGGAGAGUCUUTT-3', si-CMYC: 5'- CUGCGACGAGGAGGAGAACUUTT-3') and 2.5 µg plasmids (oe-PNMA1: HG15170-CF, SinoBiological; oe-NC: pCMV3-C-FLAG, SinoBiological) respectively. After 4 h of transfection, fresh complete culture medium with melphalam was replaced. After 48 h of transfection, the cells were collected and treated as required.

Western blot

Total cellular protein was extracted using a protein extraction kit (Beyotime) according to the manufacturer's instructions. The concentration of total protein was determined using a BCA protein assay kit (Beyotime) following the manufacturer's protocol. 40 micrograms of protein was separated from each sample by SDS-PAGE. The separated proteins was transfered to a 0.45-micron PVDF membrane (ImmobilonTM, Millipore Corp, Bedford, MA). After the membrane blocked with a rapid blocking buffer, the corresponding protein bands was cut out according to the markers, and incubated overnight at 4 °C with the appropriate primary antibody (anti-PNMA1: 13631-1-AP, Proteintech; anti-β-actin: #4970, Cell Signaling; anti-c-myc: #18583, Cell Signaling). After washed, the second antibody of anti-rabbit IgG (#7074P2, Cell Signaling) was added and incubated at room temperature for 30 min. A super-sensitive chemiluminescence (ECL) (Beyotime) detection kit was used to detect the chemiluminescent signals. Image J software was used to detect the gray value of target strip. The ratio of gray value of target protein to that of β-actin to obtain the relative expression level is calculate for normalization.

Drug dose response curves

Cells were seeded at 8,000 cells/well in 96-well clear-bottom, white-walled plates. Sixteen to twenty hours after seeding, cells were treated with drug for the indicated treatment. Cells were grown in the presence of the drug for 24 h. Cell viability was assessed using the CCK-8 assay following the manufacturer's recommendations, and the colorimetric output was measured on a Perkin Elmer Flexstation 3.0. Data were normalized to the maximum and minimum values and plotted in GraphPad Prism. The half-inhibitory concentration (IC50) values were estimated, and IC50s from replicate experiments were compared using Student's t-test.

Drug sensitivity analysis

To determine the difference in the efficacy of chemotherapeutic drugs, the "oncopredict" package was utilized to calculate IC50 values of the frequently used chemotherapeutic drugs. IC50 values for drugs were extracted from the CellMiner database, and the corresponding IC50 data for GSE229598 samples were obtained using the "oncopredict" package for training. A correlation analysis between gene expression levels and IC50 values was performed using the Spearman rank correlation coefficient.

Melphalam-resistant cell line

SO-RB50 cells were induced to be a melphalam -resistant cell line SO-RB50MR by concentration gradient increasing method. When the cell density reached 60%, the incubation was performed in the medium with 100-nmol/L of melphalam. The cells were then passed through drug-free medium for about 3 times, and the cell state gradually recovered. After repeated treatment with 100-nmol/L mephalam for 3 times, the concentration was increased according to the proliferation of surviving cells. Finally, the cells can be stably prolificated at 2500-nmol/L mephalam, indicating the successful construction of a drug-resistant cell line.

Cell counting kit 8 (CCK-8)

Cell viability was measured after treatments in 96 well plates using the CCK8 from Seven Biotech, processed according to the manufacturer's instructions and quantified on a SpectraMax microplate reader (Molecular Devices).

EdU staining

For EdU staining, growing cells were treated with EdU (2 µM) for 24 h. The cells were fixed with 10% formalin for 10 min and washed three times with PBS. EdU labeling was performed using click chemistry, where Cu (I) induced a reaction between Azide 594 (0.25 mg/mL, Beyotime) and the alkyne present in EdU. DAPI (blue)

was used to stain the nuclei. The EdU was observed under fluorescence microscope. The ratio of the number of positively stained cells to the total number of cells to obtain the relative positive rate is calculate for normalization.

Colony formation assay
 SO-RB50 cells were seeded at a density of 800 cells/well into 6-well plates. After 10 days of culture, the cells were fixed with formalin and stained with crystal violet. Under the microscope, colonies with more than 50 cells were counted.

TUNEL assay
48 h after transfection, cells in logarithmic phase were fixed with 4% paraformaldehyde at room temperature for 30 min. According to the manufacturer's instructions, TUNEL staining on cell slideswas performed using the In Situ Cell Death Detection Kit (Roche). After the cells were fixed and permeated, the TUNEL reaction mixture was reacted at 37 °C in the dark for 1 h. They were then treated with Hoechst at room temperature in the dark for 12 min. After rinsing with PBS, the apoptosis was observed under fluorescence microscope. The ratio of the number of positively stained cells to the total number of cells to obtain the relative positive rate is calculate for normalization.

Cell migration assay
The cells of each group were inoculated on a 6-well plate. When the cells were overgrown, a sterile 10 μL micropipette tip created a 1 mm wide wound. The culture was carried out at 37°C and 5% CO_2. The wound was photographed at 0 and 24 h. The migration ability of cells was analyzed by ImageJ software.

Cell invasion assay
Matrigel was added in the upper chamber with 8 μm pore size. Then, medium was added in the lower chamber. SO-RB50 cells were seeded to the upper chamber. The outer side of upper chamber was stained by crystal violet and observed under the microscope after 24 h.

PARP activity
PARP activity was measured using Trevigen's HT Colorimetric PARP/Apoptosis Assay. Cellswere grown in 96-well plates and treated with melphalan or DMSO for 24 h. The cells were washed with PBS and lysates were lysated using the provided cell extraction buffer. Tte protein concentration was estimated using the BCA Protein Assay Kit and the lysates was diluted with cell lysis buffer. The assay was performed according to the manufacturer's instructions. PARP activity was related to the absorbance of the generated colorimetric signal, which was quantified at 450 nm using SpectraMax microplate reader (Molecular Devices).

γ-H2AX staining
SO-RB50 cells were plated 24 h before the addition of melphalan. The slides were fixed with 4% formaldehyde, permeabilized with 0.5% Triton-X, and blocked overnight with 10% BSA. Following this, the slides were incubated for 4 h with anti-γH2AX antibody (1:200; Cell Signaling Technology #9718S) in 1% BSA and 0.1% Triton-X, followed by a 1-hour incubation with anti-rabbit antibody (1:1000, Abcam ab150079). The slides were digitally scanned before nuclei segmentation with the DAPI channel and γH2AX foci counting using the Find Maxima algorithm in ImageJ.

Statistical analysis
Each of experiments was repeated three times. Statistical analysis was conducted using GraphPad Prism 7 software (La Jolla, CA, USA). For comparisons between two groups, that was used, the Mann-Whitney U test for non-parametric data or Student's t-test for parametric data after verifying normality using the Shapiro-Wilk test and equality of variances using Levene's test. For multiple comparisons, that was used, one-way ANOVA followed by Tukey's post-hoc test if data met the assumptions of normality and homogeneity of variances. For non-parametric data, that was used, the Kruskal-Wallis test followed by Dunn's post-hoc test Statistical significance was indicated as follows: $*P < 0.05$, $**P < 0.01$, $***P < 0.001$. Results were derived from a minimum of three independent experiments. Error bars in all graphs represent the mean ± S.E.M.

Results
Differential gene identification
To explore genes associated with RB, two RNA high-throughput sequencing datasets were accessed, GSE97508 and GSE110811, from the GEO database. The differential analysis outcomes showed that in the GSE97508 dataset, a total of 5,346 differentially expressed genes were identified between RB samples and normal retinas, with 2,963 genes upregulated and 2,382 genes downregulated. In the GSE110811 dataset, 1,312 different genes were found to be differentially expressed, with 561 genes being upregulated and 750 genes downregulated (Supplementary Table 1). Additionally, 13 shared differentially expressed genes were identified, of which 8 genes were consistently upregulated in both datasets, and 5 genes were downregulated in both (Fig. 1A, B).

PNMA1 is upregulated in RB and promotes melphalan chemoresistance
As a frontline drug in the clinical treatment of RB, melphalan plays a crucial role in inhibiting tumor progression. Therefore, the correlation between 13 genes and melphalam sensitivity was predicated using the R package 'oncopredict'. The results showed a positive correlation between PNMA1 expression and the IC50 value of melphalam (Fig. 1C), and PNMA1 was found to be more highly expressed in RB tissues compared to normal retinal tissues (Fig. 1D, E), suggesting that high PNMA1 expression might contribute to tumor progression and
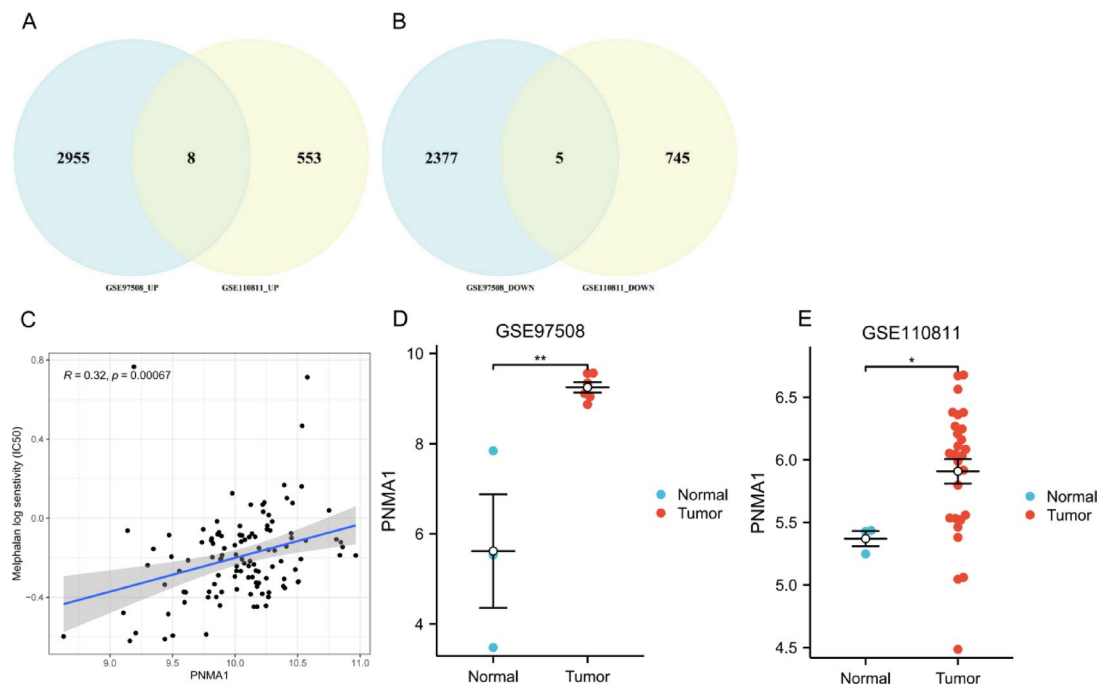
Fig. 1. PNMA1 is identified as an upregulated gene in RB and associated with melphalan drug sensitivity. **A-B** The shared differentially expressed genes between Dataset GSE97508 and Dataset GSE110811. **C.** The correlation between PNMA1 mRNA expression levels and the IC50 of melphalan. D, **E** The mRNA expression of PNMA1 between tumor and normal tissue was evaluated by GSE97508 (**D**) and GSE110811 (**E**) database. *$p < 0.05$, **$p < 0.01$.

resistance to melphalam. Statistical significance between two groups was obtained using the Wilcoxon test, with P-values adjusted via the Bonferroni method (Fig. 1D, E).

To validate these findings, PNMA1 was overexpressed in the SO-RB50 cell line with culture medium, the transfected vehicle plasmid as the control (Fig. 2A). The results demonstrated that overexpression of PNMA1 increased the IC50 value for melphalan (631.74 nmol/L) compared with the control group (585.42 nmol/L) (Fig. 2B). Next, the cells were treated with melphalan at half the concentration of IC50 for 24 h. The TUNEL experiment showed that overexpressed PNMA1 cells exhibited significantly reduced apoptosis compared with control cells (Fig. 2C). These findings indicated that PNMA1 facilitates chemoresistance to melphalam. The Student's t-test for parametric data (Fig. 2A), the Mann-Whitney U test for non-parametric data (Fig. 2C) and the two-way ANOVA followed by Bonferroni correction. (Fig. 2B) were used.

PNMA1 facilitates the proliferation, migration, and invasion of RB cells

The cells were treated with melphalan at half IC50 concentration for 24 h. Colony formation assays revealed that overexpression of PNMA1 enhanced the clonogenic capacity of RB cells compared with transfected vehicle control (Fig. 3A). CCK-8 assays and EdU staining confirmed the promoting effect of PNMA1 on RB cell proliferation and DNA synthesis rates compared with transfected vehicle control (Fig. 3B, C). These findings indicate that PNMA1 promotes the proliferation of RB cells. To further explore the impact of PNMA1 on other malignant phenotypes of RB cells, wound healing and transwell assays was conducted, which also demonstrated the facilitatory role of PNMA1 in cell migration and invasion compared with transfected vehicle control (Fig. 3D, E). In summary, PNMA1 positively regulates the proliferation and invasive abilities of RB cells. The Student's t-test for parametric data (Fig. 3A, C-E) and the two-way ANOVA followed by Bonferroni correction. (Fig. 3B) were used.

Knockdown of PNMA1 restores chemosensitivity to Melphalan in resistant cells

To further investigate the impact of PNMA1 on melphalan resistance, the resistant strain SO-RB50MR was generated. The IC50 value of the resistant strain was approximately 8 times higher than that of the wild-type cell line (Fig. 4A). Western blot results showed increased PNMA1 expression in the resistant cells with culture medium compared with the wild-type cells (Fig. 4B). Treatment of SO-RB50 and SO-RB50MR cells with melphalan at half IC50 concentration revealed significantly enhanced apoptosis in the wild-type cells, while the resistant cells exhibited higher cell viability (Fig. 4C).

PNMA1 expression was knocked down in SO-RB50MR cells with culture medium using shRNA and stable cell lines was established using lentiviral vectors (Fig. 4D). Under melphalan treatment at half IC50 concentration, the SO-RB50MR cells with PNMA1 knockdown showed increased apoptosis and reduced viability (Fig. 4E, F). Additionally, the knockdown of PNMA1 lowered the IC50 value of the SO-RB50MR cells for melphalan (Fig. 4G). These findings suggest that knocking down PNMA1 can restore chemosensitivity to melphalan
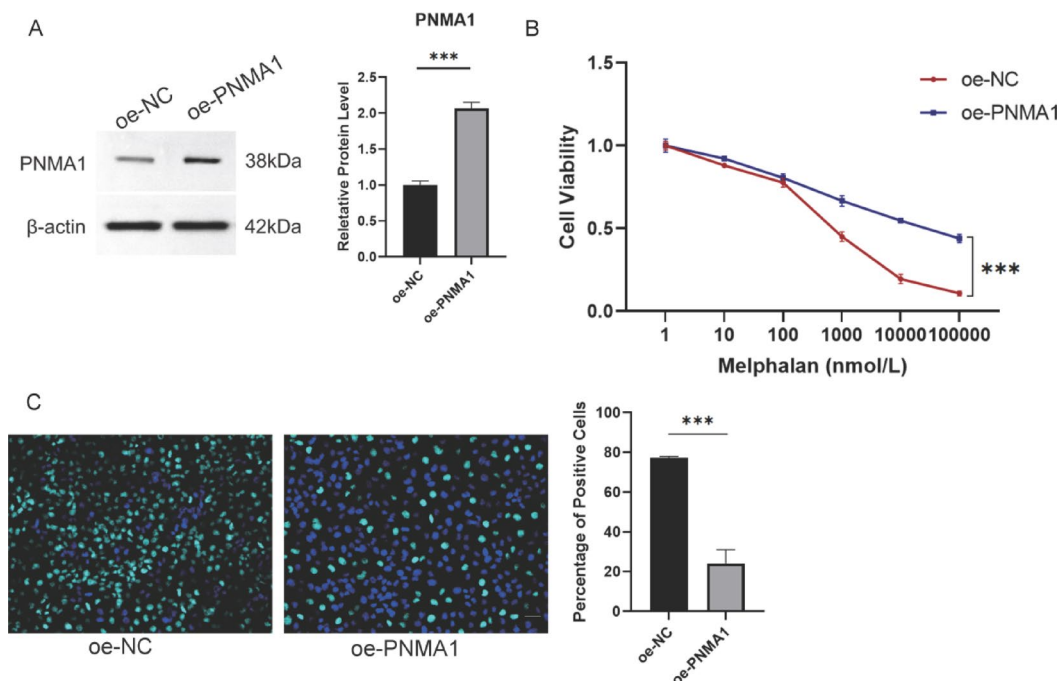
Fig. 2. Upregulation of PNMA1 expression impairs melphalan chemosensitivity. **A** Efficiency of PNMA1 overexpression. **B** The impact of PNMA1 overexpression on the half-maximal inhibitory concentration (IC50) of melphalan. **C** The effect of PNMA1 overexpression on cell apoptosis under melphalan treatment. ***$p < 0.001$.
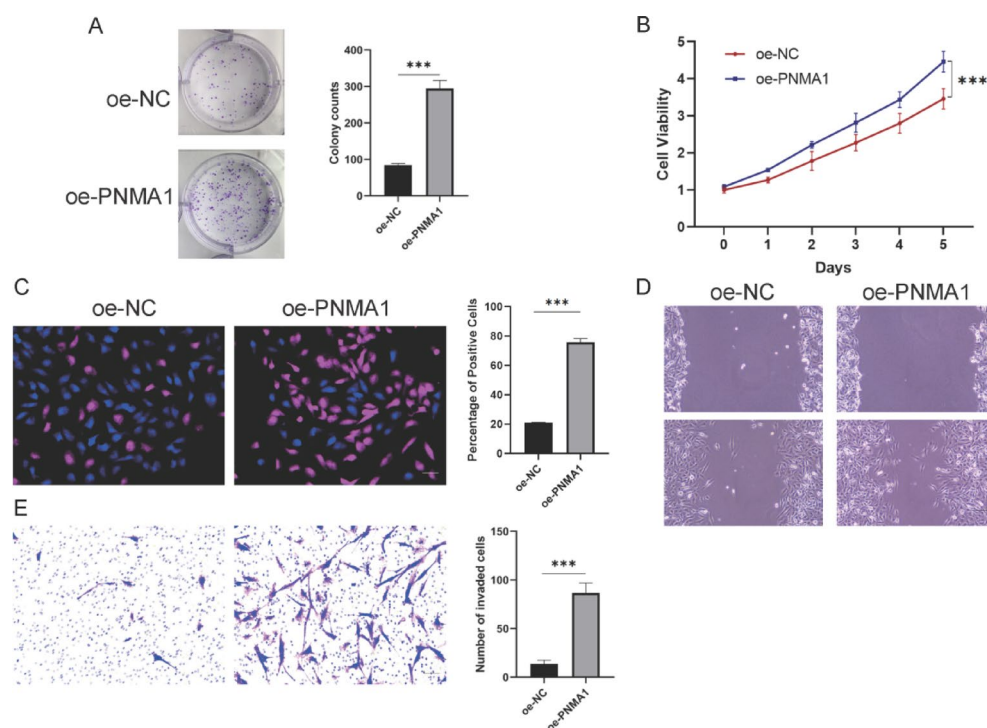
Fig. 3. Enhanced PNMA1 expression facilitates proliferation and invasion of RB cells. **A-B** Colony formation (**A**) assay and CCK8 assay(**B**) revealed that PNMA1 overexpression could increase the proliferation ability of RB cells. **C** EdU staining (red fluorescence) revealed that PNMA1 overexpression enhances DNA synthesis. D-E. Wound healing assay (**D**) and transwell assay (**E**) demonstrate that PNMA1 overexpression promotes RB cells migration and invasion. ***$p < 0.001$.
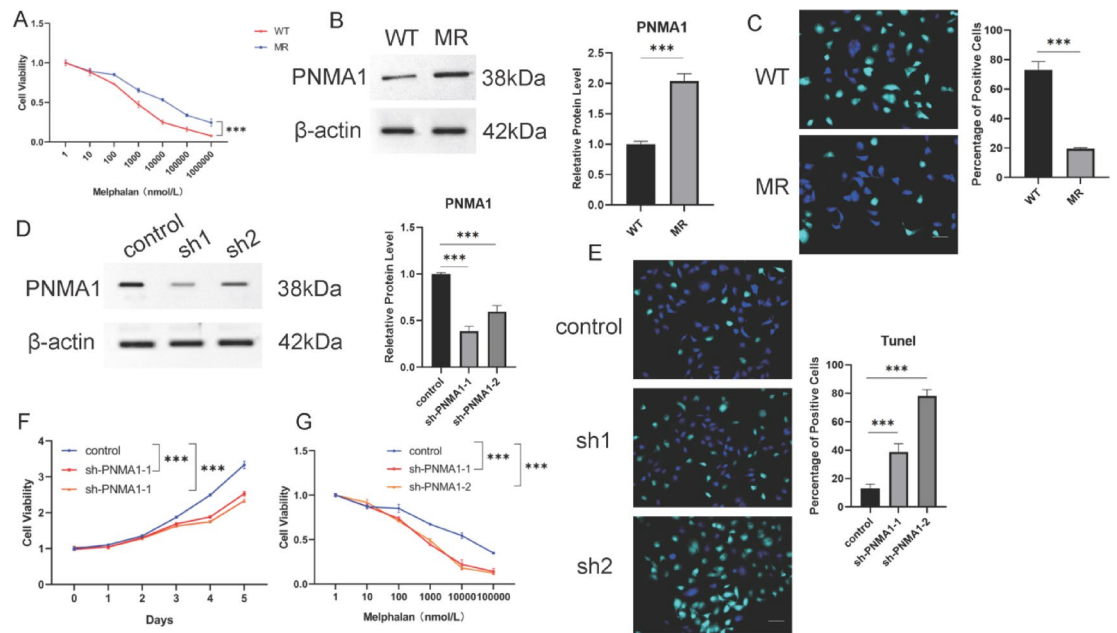
Fig. 4. Reducing PNMA1 expression can restore chemosensitivity in melphalan-resistant cells. **A** Melphalan-resistant (MR) cell lines were established. **B** PNMA1 expression is upregulated in melphalan-resistant cells. **C** MR cells exhibit enhanced anti-apoptotic properties under melphalan treatment. **D** Downregulation of PNMA1 expression in MR cells (control). **E-G** Downregulation of PNMA1 results in increased apoptosis (**E**), decreased cellular activity (**F**), and enhanced melphalan chemosensitivity (**G**) under melphalan treatment. ***$p < 0.001$.

in resistant cells. The Student's t-test for parametric data (Fig. 4B, D-E), the Mann-Whitney U test for non-parametric data (Fig. 4C) and the two-way ANOVA followed by Bonferroni correction. (Fig. 4A, F-G) were used.

PNMA1 mediates Melphalan chemoresistance through enhanced DNA damage repair

As a DNA alkylating agent, melphalan's primary anticancer mechanism involves inducing DNA damage in tumors. PNMA1 might contribute to melphalan chemoresistance by promoting DNA damage repair. The results showed that shPNMA1 SO-RB50MR cells exhibited higher γH2AX levels and lower PARP activity compared to shNC SO-RB50MR control cells with culture medium (Fig. 5A, B), indicating that PNMA1 knockdown exacerbated DNA damage and inhibited DNA repair. Conversely, overexpression of PNMA1 in the SO-RB50 wild-type cell line led to increased PARP activity and lower γH2AX levels compared with transfected vehicle control with melphalan at half IC50 concentration (Fig. 5C, D), suggesting that PNMA1 overexpression promoted DNA damage repair. These findings collectively suggest that PNMA1 mediates melphalan chemoresistance through its role in enhancing DNA damage repair. The Student's t-test for parametric data (Fig. 5A-D).

PNMA1 enhances DNA damage repair by upregulating c-myc, thereby contributing to RB chemoresistance

To further investigate the mechanism by which PNMA1 affects DNA damage repair, GSEA analysis on PNMA1 was performed using the GSE229598 dataset. The GSEA results showed a positive correlation between PNMA1 and the 'HALLMARK_MYC_TARGETS_V1' and 'HALLMARK_MYC_TARGETS_V2' pathways (Fig. 6A). In the SO-RB50 cells, c-myc gene expression was upregulated after overexpressing PNMA1 compared with transfected vehicle cells, while in the shPNMA1 SO-RB50MR cell line, c-myc expression was downregulated after knocking down PNMA1 compared to shNC SO-RB50MR control cells, cells were treated with culture medium (Fig. 6B). Notably, c-myc expression was higher in SO-RB50MR cells compared to the wild-type SO-RB50 cells (Fig. 6B). Upon knocking down c-myc in SO-RB50MR cells, PNMA1 expression remained unchanged, but γH2AX levels increased, and PARP activity decreased compared to shNC SO-RB50MR control cells with culture medium (Fig. 6C-E). Next, c-myc was knocked down while overexpressing PNMA1 in SO-RB50 cells and each group of cells was simultaneously treated with melphalam at half IC50 concentration. Compared to the PNMA1overexpression group, the group with both PNMA1 overexpression and c-myc knockdown showed increased apoptosis, reduced cell viability, elevated γH2AX, and decreased PARP activity (Fig. 6F-H). Additionally, the combination of PNMA1 overexpression and c-mycknockdown lowered the IC50 of melphalan (Fig. 6I). This suggests that knocking down c-myc impairs PNMA1-mediated DNA damage repair and chemoresistance. Collectively, these results indicate that PNMA1 may promote DNA damage repair by upregulating c-myc, thereby contributing to chemoresistance in RB. The Student's t-test for parametric data (Fig. 6B-E), one-way ANOVA followed by Tukey's post-hoc test for parametric data (Fig. 6H), Kruskal-Wallis
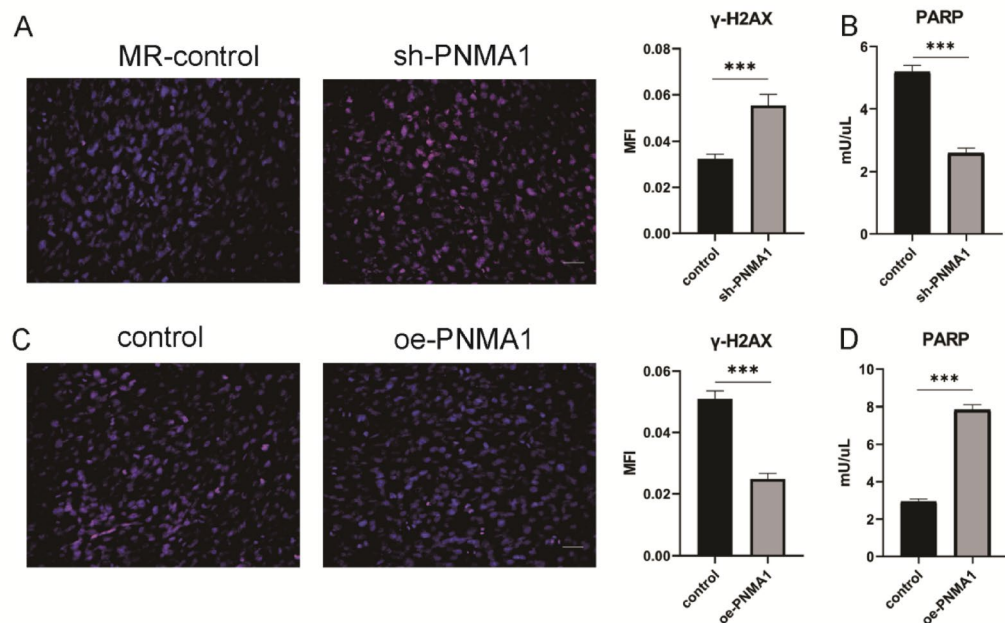
Fig. 5. PNMA1 affects DNA damage repair. **A-B** Downregulation of PNMA1 increased DNA damage (**A**) and decreased DNA repair capability (**B**). **C-D** Upregulation of PNMA1 decreased DNA damage (**C**) and increased DNA repair capability (**D**). ***$p < 0.001$.

test followed by Dunn's post-hoc test for parametric data (Fig. 6F, G), and the two-way ANOVA followed by Bonferroni correction. (Fig. 6I) were used.

Discussion

PNMA1 wais initially discovered in the serum of patients with neuroendocrine tumors of the nervous system[15]. At present, PNMA1 has been confirmed to play an important role in the malignant process of a variety of tumors. However, the role of PNMA1 in RB remains unclear. A study suggests that PNMA1 regulates the WNT/β-catenin pathway to facilitate EMT in hepatocellular carcinoma cells[12]. Previous study found that PNMA1 knockdown inhibits the migration, invasion, proliferation and proliferation of osteosarcoma cells[16]. Furthermore, inhibition of PNMA1 expression promotes apoptosis and reduces cell viability in pancreatic ductal adenocarcinoma[11]. This study found that PNMA1 facilitates proliferation, migration, and invasion of RB cells, which is consistent with the above conclusions. Therefore, PNMA1 is suggested its potential as a driver molecule in RB tumor progression.

Chemotherapy advancements have improved the chances of preserving vision in young patients with retinoblastoma[17]. Melphalan, a frontline chemotherapy drug for RB, is commonly used[18,19], but resistance remains a significant barrier to treatment success[20]. Therefore, identifying targets to overcome melphalan resistance is crucial.

In this study, elevated PNMA1 expression was observed in RB tumors compared to normal tissue. Bioinformatics analysis revealed that high PNMA1 expression might contribute to RB tumor cell resistance, and experiments confirmed that PNMA1 levels were significantly higher in resistant cells than in wild-type ones. PNMA1 mediated chemoresistance in RB cells, and downregulating PNMA1 effectively reversed melphalam resistance. Melphalan exerted its anti-tumor activity by forming cross-links with DNA, causing DNA damage[21]. Consequently, PNMA1's impact on DNA damage repair was investigated. PNMA1 was found to enhance DNA repair, which may be the main mechanism for promoting chemotherapy resistance. Therefore, PNMA1 may be a therapeutic target for RB.

GSEA of mRNA-seq data from the GEO database in the PNMA1-high RB group showed enrichment of the 'HALLMARK_MYC_TARGETS_V1' and 'HALLMARK_MYC_TARGETS_V2' pathways. c-myc, a transcription factor encoded by the oncogene MYC, plays a critical role in cell growth, proliferation, and metabolism[22]. c-myc is implicated in various tumor development processes[19,23–27]. Numerous studies confirm that increased c-myc levels can upregulate transcription via RNA polymerase I-III, promoting replication, RNA processing, and translation[28–34]. During DNA damage, c-myc accumulates around stalled replication forks or promoters, recruiting other proteins to form a complex that aids DNA repair[35,36]. These findings suggest that PNMA1 regulates the expression of c-myc in RB cells. PNMA1 may enhance DNA repair by upregulating c-myc expression, and downregulating c-myc protein levels effectively counteracts PNMA1's promotion of DNA repair ability and chemoresistance. However, due to the limitations of this study, the role of PNMA1 in tumor tissues and vitreous seeds has not been studied, and relevant studies may be considered in the future.
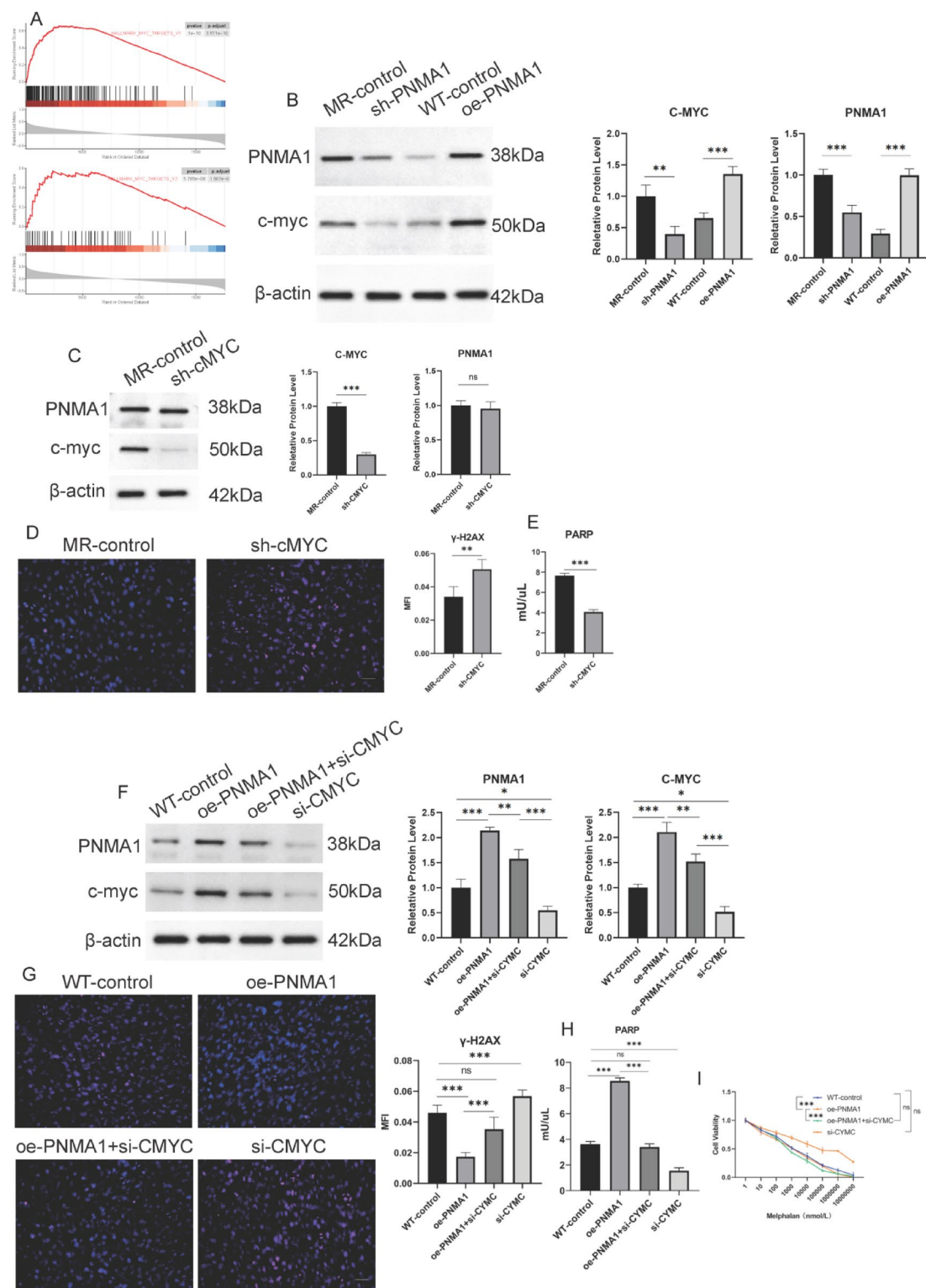
Fig. 6. PNMA1 regulates c-myc to affect DNA damage repair. **A** Gene Set Enrichment Analysis (GSEA) results indicate that PNMA1 is associated with the c-myc signaling pathway. **B** Upregulation or downregulation of PNMA1 leads to changes in c-myc protein levels. **C-E** Downregulation of c-myc in MR cells (**C**) results in increased DNA damage (**D**) and reduced repair (E). F-I. Simultaneous upregulation of PNMA1 and downregulation of c-myc (**F**) results in increased DNA damage (**G**), reduced DNA repair (H), and enhanced melphalan chemosensitivity (**I**). $**p < 0.01$, $***p < 0.001$, ns, not significant.

Conclusion

PNMA1 is an oncogene in RB that may promote DNA repair by upregulating c-myc expression, thereby mediating melphalan chemoresistance. These findings suggest that PNMA1 promotes in the development of RB and that PNMA1 may be a potential therapeutic target for RB.

Data availability

The datasets used and/or analysed during the current study available from the corresponding author on reasonable request.

References

1. The Global Retinoblastoma. Outcome study: a prospective, cluster-based analysis of 4064 patients from 149 countries. *Lancet Glob Health*. **10** (8), e1128–e1140 (2022).
2. Chawla, B. et al. Clinical presentation and survival of retinoblastoma in Indian children. *Br. J. Ophthalmol.* **100** (2), 172–178 (2016).
3. Kaliki, S. et al. Bilateral advanced (group D or E) intraocular retinoblastoma: outcomes in 72 Asian Indian patients. *Eye (Lond)*. **33** (8), 1297–1304 (2019).
4. Shields, C. L. et al. Factors predictive of recurrence of retinal tumors, vitreous seeds, and subretinal seeds following chemoreduction for retinoblastoma. *Arch. Ophthalmol.* **120** (4), 460–464 (2002).
5. Zhu, X. et al. The FoxM1-ABCC4 axis mediates carboplatin resistance in human retinoblastoma Y-79 cells. *Acta Biochim. Biophys. Sin (Shanghai)*. **50** (9), 914–920 (2018).
6. Chan, H. S. et al. Multidrug resistance protein (MRP) expression in retinoblastoma correlates with the rare failure of chemotherapy despite cyclosporine for reversal of P-glycoprotein. *Cancer Res.* **57** (12), 2325–2330 (1997).
7. Balla, M. M., Vemuganti, G. K., Kannabiran, C., Honavar, S. G. & Murthy, R. Phenotypic characterization of retinoblastoma for the presence of putative cancer stem-like cell markers by flow cytometry. *Invest. Ophthalmol. Vis. Sci.* **50** (4), 1506–1514 (2009).
8. Pang, S. W., Lahiri, C., Poh, C. L. & Tan, K. O. PNMA family: protein interaction network and cell signalling pathways implicated in cancer and apoptosis. *Cell. Signal.* **45**, 54–62 (2018).
9. Schüller, M., Jenne, D. & Voltz, R. The human PNMA family: novel neuronal proteins implicated in paraneoplastic neurological disease. *J. Neuroimmunol.* **169** (1–2), 172–176 (2005).
10. Chen, H. L. & D'Mello, S. R. Induction of neuronal cell death by paraneoplastic Ma1 antigen. *J. Neurosci. Res.* **88** (16), 3508–3519 (2010).
11. Jiang, S. H. et al. PNMA1 promotes cell growth in human pancreatic ductal adenocarcinoma. *Int. J. Clin. Exp. Pathol.* **7** (7), 3827–3835 (2014).
12. Liu, P., Chen, B., Gu, Y. & Liu, Q. PNMA1, regulated by miR-33a-5p, promotesproliferation and EMT in hepatocellular carcinoma by activating the Wnt/β-catenin pathway. *Biomed. Pharmacother.* **108**, 492–499 (2018).
13. Leek, J., Johnson, W., Parker, H., Jaffe, A. & Storey, J. The Sva package for removing batch effects and other unwanted variation in high-throughput experiments. *Bioinf. (Oxford England)*. **28**, 882–883 (2012).
14. Ritchie, M. et al. Limma powers differential expression analyses for RNA-sequencing and microarray studies. *Nucleic Acids Res.* **43**, e47 (2015).
15. Dalmau, J. et al. Ma1, a novel neuron- and testis-specific protein, is recognized by the serum of patients with paraneoplastic neurological disorders. *Brain* **122** (Pt 1), 27–39 (1999).
16. Wei, X., Dan, L., Xi, C., Leiting, L. & Weihong, X. LncRNA JPX modulates malignant progress of osteosarcoma through targeting miR-33a-5p and PNMA1 regulatory loop. *Transl Oncol.* **25**, 101504 (2022).
17. Fabian, I. D. et al. The management of retinoblastoma. *Oncogene* **37** (12), 1551–1560 (2018).
18. Redondo-Villanueva, M. & Mercado, G. Intravitreal Melphalan for persistent retinoblastoma vitreous seeds. *GMS Ophthalmol. Cases*. **12**, Doc03 (2022).
19. Jiang, K. et al. Topical instillation of cell-penetrating peptide-conjugated Melphalan blocks metastases of retinoblastoma. *Biomaterials* **284**, 121493 (2022).
20. Lu, D., Yang, C., Zhang, Z., Cong, Y. & Xiao, M. Knockdown of Linc00515 inhibits multiple myeloma autophagy and chemoresistance by upregulating miR-140-5p and downregulating ATG14. *Cell. Physiol. Biochem.* **48** (6), 2517–2527 (2018).
21. Dhillon, S. Melphalan flufenamide (Melflufen): first approval. *Drugs* **81** (8), 963–969 (2021).
22. Das, S. K., Lewis, B. A. & Levens, D. MYC: a complex problem. *Trends Cell. Biol.* **33** (3), 235–246 (2023).
23. Wasylishen, A. R. & Penn, L. Z. Myc: the beauty and the Beast. *Genes Cancer*. **1** (6), 532–541 (2010).
24. Spencer, C. A. & Groudine, M. Control of c-myc regulation in normal and neoplastic cells. *Adv. Cancer Res.* **56**, 1–48 (1991).
25. Wu, S. et al. Circular EcDNA promotes accessible chromatin and high oncogene expression. *Nature* **575** (7784), 699–703 (2019).
26. Wu, S., Bafna, V., Chang, H. Y. & Mischel, P. S. Extrachromosomal DNA: an emerging hallmark in human Cancer. *Annu. Rev. Pathol.* **17**, 367–386 (2022).
27. Adey, A. et al. The haplotype-resolved genome and epigenome of the aneuploid HeLa cancer cell line. *Nature* **500** (7461), 207–211 (2013).
28. Dominguez-Sola, D. et al. Non-transcriptional control of DNA replication by c-Myc. *Nature* **448** (7152), 445–451 (2007).
29. Dominguez-Sola, D. & Gautier, J. MYC and the control of DNA replication. *Cold Spring Harb Perspect. Med.* **4** (6), a014423 (2014).
30. Cowling, V. H. & Cole, M. D. The Myc transactivation domain promotes global phosphorylation of the RNA polymerase II carboxy-terminal domain independently of direct DNA binding. *Mol. Cell. Biol.* **27** (6), 2059–2073 (2007).
31. Cole, M. D. & Cowling, V. H. Transcription-independent functions of MYC: regulation of translation and DNA replication. *Nat. Rev. Mol. Cell. Biol.* **9** (10), 810–815 (2008).
32. Campbell, K. J. & White, R. J. MYC regulation of cell growth through control of transcription by RNA polymerases I and III. *Cold Spring Harb Perspect. Med.* **4** (5), a018408 (2014).
33. Bowling, E. A. et al. Spliceosome-targeted therapies trigger an antiviral immune response in triple-negative breast cancer. *Cell* **184** (2), 384–403e21 (2021).
34. Baluapuri, A., Wolf, E. & Eilers, M. Target gene-independent functions of MYC oncoproteins. *Nat. Rev. Mol. Cell. Biol.* **21** (5), 255–267 (2020).
35. Hamperl, S. & Cimprich, K. A. Conflict resolution in the genome: how transcription and replication make it work. *Cell* **167** (6), 1455–1467 (2016).
36. Solvie, D. et al. MYC multimers shield stalled replication forks from RNA polymerase. *Nature* **612** (7938), 148–155 (2022).

Author contributions

Longge Sun and Zhaokang Xu contributed to the conception of the study. Xin Zhang and Xing Du contributed significantly to the data analysis and study preparation. Guanghui Li performed the data analyses and wrote the study. Yuanyuan Guo helped perform the analysis with constructive discussions. All authors have read and approved the final study.

Declarations

Competing interests

The authors declare no competing interests.

Ethics statement

This study did not involve human or animal subjects; therefore, ethics committee approval is not applicable.

Additional information

Supplementary Information The online version contains supplementary material available at https://doi.org/10.1038/s41598-025-12206-0.

Correspondence and requests for materials should be addressed to Y.G.

Reprints and permissions information is available at www.nature.com/reprints.

Publisher's note Springer Nature remains neutral with regard to jurisdictional claims in published maps and institutional affiliations.